Materials Science and Engineering A 527 (2009) 334–338

Contents lists available at ScienceDirect

Materials Science and Engineering A

journal homepage: www.elsevier.com/locate/msea

Study on microstructures and mechanical properties of short-carbon-fiber-reinforced SiC composites prepared by hot-pressing

Xiulan He[a,*], Yingkui Guo[a], Zemin Yu[a], Yu Zhou[b], Dechang Jia[b]

[a] Department of Materials Science and Engineering, Harbin University of Science and Technology, 52 Xuefu Road, Nangang District, Harbin 150040, China
[b] Department of Materials Science and Engineering, Harbin Institute of Technology, Harbin 150001, China

ARTICLE INFO

Article history:
Received 18 April 2009
Received in revised form 2 August 2009
Accepted 4 August 2009

Keywords:
Short-carbon-fiber-reinforced SiC composites
Polycarbosilane
Hot-pressing
Microstructure
Mechanical property

ABSTRACT

Short-carbon-fiber-reinforced silicon carbide composites were prepared by hot-pressing with SiC powder, Polycarbosilane as precursor polymer and $MgO–Al_2O_3–Y_2O_3$ as sintering additives. The phase composition, microstructure and mechanical properties of the composites with different Polycarbosilane content were investigated. The results showed that, dense composites could be prepared at a relatively low temperature of 1800 °C via the liquid-phase-sintering mechanism and the highest mechanical property was obtained for the composites with 20 wt.% PCS and 8 wt.% sintering additives. The amorphous interphase formed during sintering process in the composites not only contributed to the densification of the composites, but also improved the fiber–matrix bonding. The nano-silicon carbide derived from Polycarbosilane, could also play a role of improving the relative density of the composites.

© 2009 Elsevier B.V. All rights reserved.

1. Introduction

Silicon carbide (SiC) ceramic has attracted considerable interest for applications in wide temperature range due to its excellent properties at elevated temperatures, such as strength and modulus, creep resistance and chemical stability [1]. Over the past years, much attention has been focused on continuous fiber-reinforced SiC-based composites.

These composites could be fabricated by chemical vapor infiltration (CVI), polymer infiltration and pyrolysis (PIP) and melt infiltration (MI) methods [2–7]. However, because of the lengthy applied cycles, much time is required in those methods to produce a dense component, which may result in high-cost for even simple shapes.

At present, because of easy adaptability to conventional manufacturing techniques and low cost of fabrication, short-fiber-reinforced composites will increasingly be used in a wide range of application [8]. So it is more important to understand short-fiber-reinforced composites mechanical properties, which depend strongly on the interfacial bonding between fiber and matrix. It is well known that the fiber/matrix interphase characteristics played a key role in controlling mechanical properties of the fiber-reinforced composites. In particular, the interphase in fiber/ceramic composite not only plays the role of transferring the load between fiber and matrix, but also affects the fracture behavior of the composites [9].

Polycarbosilane (PCS) had been widely used as a precursor polymer for SiC fibers and fiber-reinforced composites. The technique of fabricating ceramics by pyrolysis of organometallic polymers has many possibilities in producing new materials. During hot-pressing, the pyrolysis products from PCS mainly consist of some β-SiC microcrystalline as well as some amorphous Si–O–C, SiO_2 and free C. The reaction of sintering additives with the pyrolysis products from PCS can form the liquid-phase interphase, which was distributed to the grain boundaries and fiber/matrix interphase mainly in an amorphous form after sintering. So the degradation of the carbon fibers, which was caused by high sintering temperature could be avoided, and it was possible to obtain desire interfacial bonding between fiber and matrix. In addition, the nano-SiC derived from PCS could also play a role of improving the relative density of the composites [10]. So far, most works have been published concerning the continuous fiber-reinforced SiC-based composites [11–13]. However, report on the short-carbon-fiber-reinforced SiC composites with PCS as precursor polymer is rather limited and the effect of PCS on the property of the composites is less clear.

* Corresponding author. Tel.: +86 451 86392500; fax: +86 451 86392501.
E-mail address: hexiulan1973@yahoo.com.cn (X. He).

0921-5093/$ – see front matter © 2009 Elsevier B.V. All rights reserved.
doi:10.1016/j.msea.2009.08.004

In the present work, short-carbon-fiber-reinforced SiC composites with PCS as precursor polymer and $MgO–Al_2O_3–Y_2O_3$ as sintering additives were prepared by hot-pressing. The effects of PCS content on microstructures and mechanical properties of the composites were investigated.

2. Experimental procedure

2.1. Fabrication of composites

PCS (National University of Defense Technology, Changsha, China) was selected as the precursor, whose mean molecular weight and melting point were 1375 and 215–236 °C, respectively. Commercially available β-SiC (Central Iron & Steel Research Institute, Beijing, China) was used as the starting powder, with an average particle size of ~0.8 μm. MgO, Al_2O_3 and Y_2O_3 (purity >99.5%, Shanghai Factory of Chemical Reagent, China) were chosen as the sintering additives and a standard additive composition of 67:16:17 (mol.%) $MgO:Al_2O_3:Y_2O_3$ was used throughout. The average tensile strength and density of the carbon fiber used in this study (Model TX-3, PAN-precursor, Elastic modulus = 220 GPa, Jilin Carbon Group Company Ltd., China) was 3.84 GPa and 1.76 g/cm^3, respectively. For all materials prepared, the carbon fiber volume fraction of the composites was kept at about 20 vol.%. The compositions of materials are shown in Table 1.

The starting powder for the matrix components was prepared by ball-milling of a submicron β-SiC powder, PCS and various kinds of sintering additives for 24 h in absolute ethanol using ZrO_2 balls. The short-carbon-fibers (4–6 mm) were dispersed 0.5 h in absolute ethanol using the ultrasonic dispersing system (SKQ-2200), then the SiC-PCS-additives solution was added to the suspension of fibers. This suspension was further dispersed 0.5 h in the ultrasonic dispersing system to obtain the final slurry. After drying, the prepared mixtures were prepressed into compacts in a graphite die. Finally, the compacts were hot pressed at 1800 °C under a pressure of 20 MPa in Ar atmosphere (0.5 atm) for 1 h.

2.2. Characterization of composites

The bulk densities of the samples were measured according to Archimedes' principle with deionized water as immersion medium. The flexural strength was determined using a three-point-bending test on 3 mm × 4 mm × 36 mm bar with a span of 30 mm and a cross-head speed of 0.5 mm/min. For fracture toughness, single-edge-notched-beam (SENB) test was used with a cross-head speed of 0.05 mm/min and a span of 16 mm. The samples were 2 mm × 4 mm × 20 mm^3 with the notch depth to samples thickness of ~0.25 mm. For all the tests, five or six specimens were tested for each batch of composites.

Characterization of the microstructure was performed by transmission electron microscopy (TEM, Philips CM-12). In addition, the samples for TEM were prepared using the procedures for ceramics. First, thin foils with a diameter of 3 mm were cut and mechanically ground to a thickness of 50–60 μm, then further thinned to about 20 μm by dimpling, followed by ion-thing (Gatan-600) until perforation. The fracture surfaces of the samples were observed by scanning electron microscopy (SEM, FEI Sirion, Holland). The phases contained in the samples were identified by X-ray diffractometry (XRD, D/max-rB, Japan) with Cu Kα radiation.

Table 1
The compositions of the composites.

Sample	Additives (wt.%)	PCS (wt.%)
SO8P0	8	0
SO8P10	8	10
SO8P20	8	20
SO8P30	8	30
SO8P40	8	40

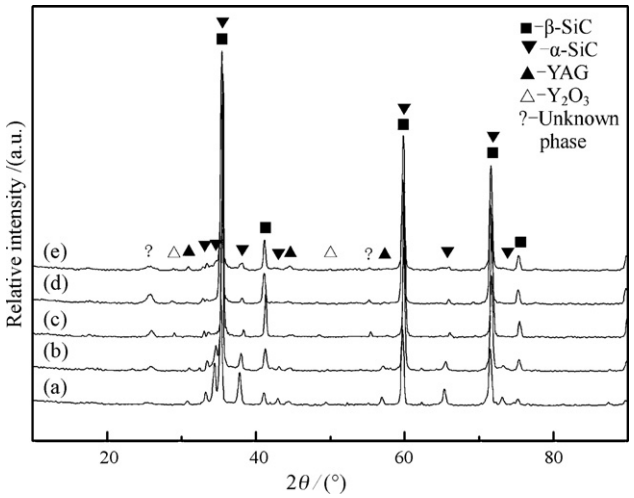


Fig. 1. XRD patterns of the composites: (a) SO8P0; (b) SO8P10; (c) SO8P20; (d) SO8P30; (e) SO8P40.

3. Results and discussion

3.1. XRD patterns of the composites

Fig. 1 illustrates XRD patterns of the composites. The results of XRD show that β-SiC was identified as a main phase for all of samples. In addition, α-SiC, Y_2O_3 and $Y_3Al_5O_{12}$ (YAG) were also detected in the XRD results. α-SiC detected by XRD showed that the starting powder β-SiC might have undergone a phase transformation from β to α.

From the presence of YAG in this present work, it could be concluded that the sintering mechanism in the composites is the liquid-phase-sintering. Liquid-phase-sintered fiber-reinforced SiC composite could reduce sintering temperature and avoid the degeneration of the carbon fiber. In addition, according to the $Al_2O_3–Y_2O_3$ phase diagram, there are three eutectic phases between Al_2O_3 and Y_2O_3, they are YAG ($Y_3Al_5O_{12}$), YAP ($YAlO_3$) and YAM ($Y_4Al_2O_9$). YAG is the lowest eutectic phase and its melting point is about 1760 °C. It can improve sinterability and interfacial strength between the fiber and matrix [14]. Therefore, the YAG formed in this study would be beneficial to improve mechanical property of composites.

In addition, there were some residual Y_2O_3 in the composites. One reason might be that there was no reaction between Y_2O_3 and SiC below 2000 °C, the other reason was the amount of Al_2O_3 was about equal to that of Y_2O_3.

3.2. Microstructures of composites

Typical microstructures of the composite with different PCS content are represented in Fig. 2. It was apparent that several types of interphases were identified in the composites. One was the direct contact between the fiber and matrix (Fig. 2(a)). In generally, the direct contact between the fiber and matrix in the carbon fiber-reinforced composites will lead to the degeneration of carbon fiber at high sintering temperature, and the toughing mechanism such as interfacial debonding, fiber pullout to operate cannot be realized in those composites. So the direct contact interface between the fiber and matrix is often characterized as strong, and the strong interfacial debonding tend to allow a crack to propagate straightly

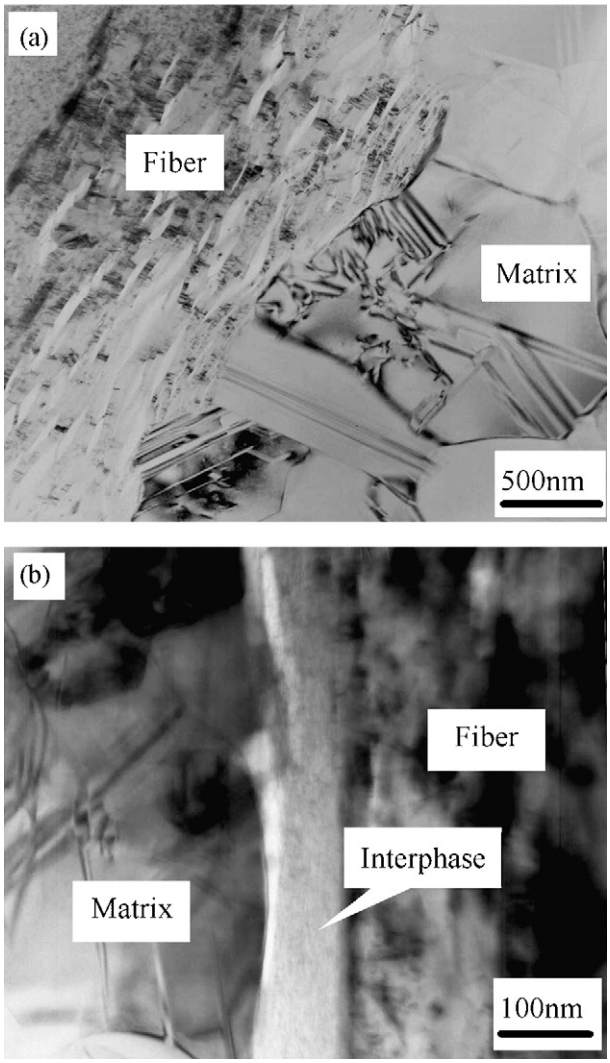


Fig. 2. TEM images of the C_f/SiC composites: (a) the direct contact between the fiber and matrix of the SO8P10 composites; (b) the amorphous interphase between the fiber and matrix of the SO8P20 composites.

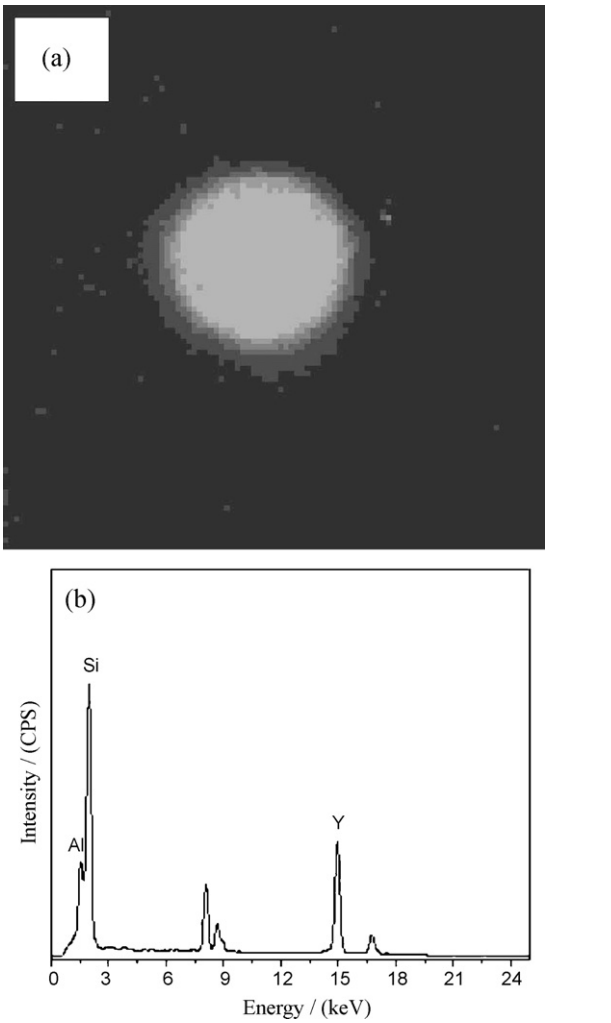


Fig. 3. (a) SAD-pattern of the amorphous interphase of the SO8P20 composites; (b) EDS-pattern of the amorphous interphase of the SO8P20 composites.

through the fibers, resulting in lower mechanical property [15]. This kind of direct contact was so much present in the SO8P0 and SO8P10 composites that the composites would exhibit a brittle failure mode and the mechanical properties of the composite were lower than other composites with more PCS as shown later in this article.

The second was the amorphous interphase between the fiber and matrix in the composites with more PCS shown in Fig. 2(b). Its SAD-pattern and EDS-pattern are given in Fig. 3(a) and (b). It can be evidenced from the SAD-pattern that the interphase was amorphous. In addition, the EDS characterization showed that the amorphous interphase consisted Y and Al elements. It has been documented that in the composites with PCS as precursor polymer and Y_2O_3, Al_2O_3 as sintering additive prepared by hot-pressing at temperature above 1750 °C, a liquid-phase formed through the reaction of Y_2O_3, Al_2O_3 with the pyrolysis products from the PCS and the liquid-phase almost distributed at the fiber–matrix interphase mainly in an amorphous form after sintering [16]. It has been proved that the fiber/matrix interphase is considered to be one of the most important factors influencing the mechanical properties of the composites, suitable fiber/matrix interfacial can facilitate toughening mechanism such as interfacial debonding, fiber pull-out to operate, but a strong interfacial bonding tend to allow a crack to propagate straightly through the fibers, resulting in lower mechanical property [17]. Therefore, the amorphous interphase formed in this study was a relatively weak interphase compared with the direct contact interphase, and the amorphous interphase not only avoided the direct contact of the fibers with matrix, but also improved the fiber/matrix bonding and realized the pullout function of carbon fiber. So it could be concluded that the composites with suitable content of PCS and sintering additive could form amorphous interphase, and exhibited easier densification and higher mechanical properties.

The third is the interphase between the starting β-SiC and nano-crystals β-SiC derived from PCS. The TEM image of nano-SiC is shown in Fig. 4. From the TEM observation, the matrix could be observed to be mainly composed of some big SiC grains, and many small SiC grains almost existed in the voids of the matrix. As massive (10-40 wt.%) PCS have been added to the composites, those nano-SiC might derived from the pyrolysis products from PCS. As shown, the average grain size of PCS-derived SiC was as small as about 300 nm, and those nano-crystals SiC not only lied on the surface of the particles of starting powder β-SiC but also existed between the carbon fiber, so they could play a role of filling up the void and improve the relative density of the composites. In addition, the TEM results also showed that a small amount of α-SiC was found in the composite, which was consistent with the XRD results. The TEM image and diffraction pattern of α-SiC are shown in Fig. 5. The

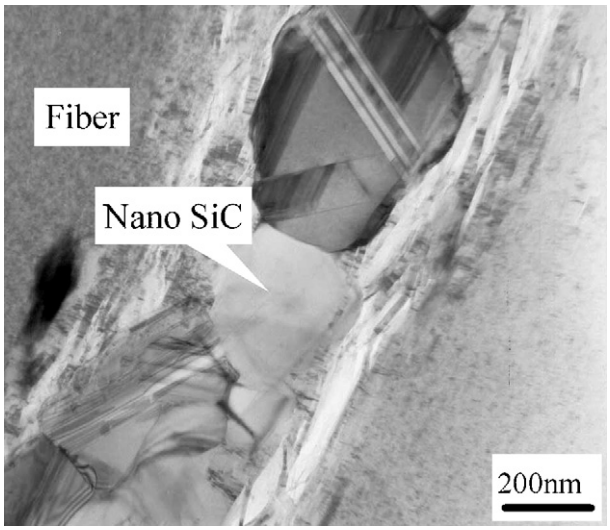


Fig. 4. TEM image of nano-SiC existed between the carbon fiber.

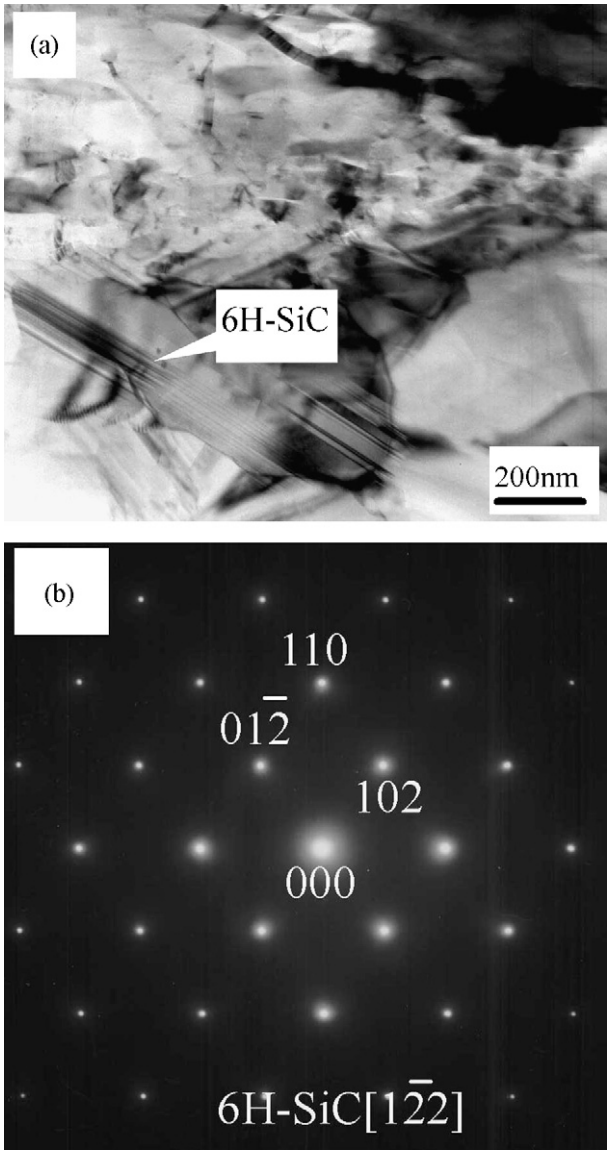


Fig. 5. (a) TEM image of 6H–SiC; (b) diffraction pattern of 6H–SiC.

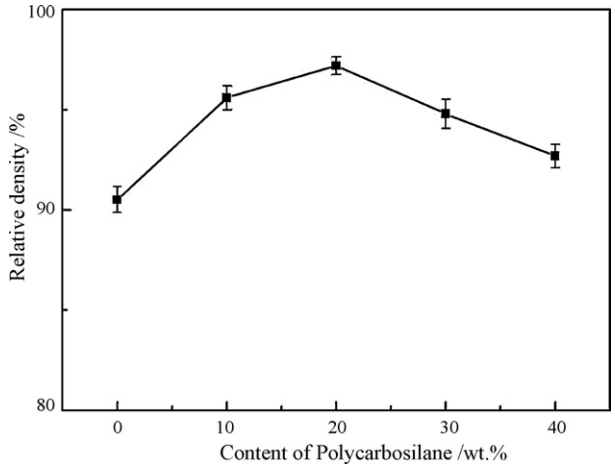


Fig. 6. Relative density of the composites as a function of Polycarbosilane content.

α-SiC crystals were plate-like, and could play a role of reinforcing agents similar to the whiskers.

From these results, it can be concluded that suitable amount of PCS and sintering additives are beneficial to form the fiber/matrix interphase and to improve mechanical properties of the composites.

3.3. Mechanical properties of composites

The relative density of the composites as a function of PCS content is given in Fig. 6. As shown, the relative density firstly increased, and then decreased with increasing PCS content. The highest relative density was obtained for the SO8P20 composite is probably due to the formation of proper content of liquid-phase. It was reported that the pyrolysis products of PCS at 1000 °C in Ar included SiO_2 (4.7 wt.%) and free C (12.3 wt.%) besides SiC (80.6 wt.%). The shrinkage of PCS during processing and the free carbon would result in lower relative density [18]. Due to excessive PCS were added to the SO8P30 and SO8P40 composite, lower relative density was exhibited because of the shrinkage of PCS during processing in those composites.

The mechanical properties of composites are given in Fig. 7. As shown, the SO8P0 and SO8P10 composites exhibited much lower mechanical properties, which was attributed to the lower relative density and the strong fiber–matrix interfacial bonding. In addition, the bending strength was improved with increasing content of PCS,

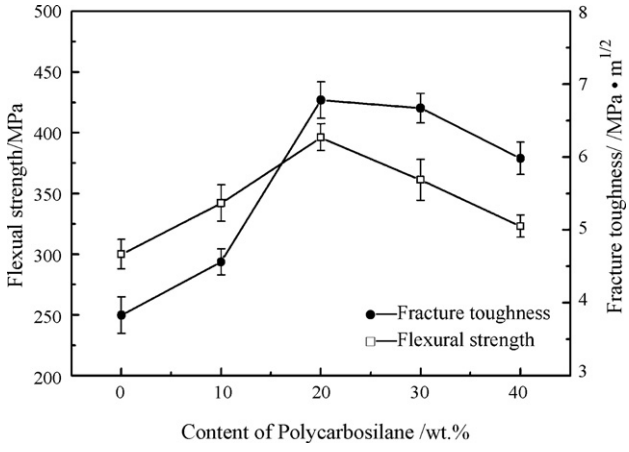


Fig. 7. Flexural strength and fracture toughness as a function of Polycarbosilane content.

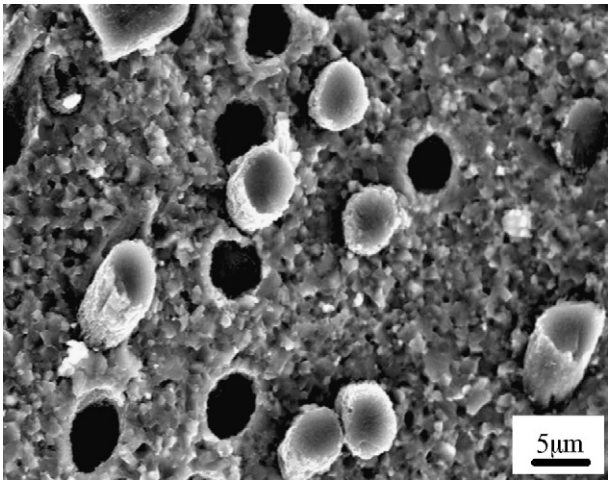


Fig. 8. SEM micrographs of fracture surfaces of the SO8P20 composites.

the highest flexural strength, 395.5 MPa and the highest fracture toughness, 6.8 MPa $m^{1/2}$ were also obtained for the SO8P20 composites. This result indicated that 20 wt.% PCS and 8 wt.% sintering additives were suitable to form appropriate amount amorphous interphase at this sintering temperatures, which was benefit for the densification of the composites. It is well known that the mechanical properties of fiber-reinforced ceramic composites depend not only on the properties of fiber and matrix and the processing conditions, but also on the fiber/matrix interfacial characteristics which play a major role in controlling the properties of composites [19]. In this study a desirable fiber/matrix interfacial bonding in the SO8P20 composites was also obtained, which facilitated the debonding and pullout of the fibers, so the highest mechanical properties belonged to the SO8P20 composites.

The decrease in bending strength and fracture toughness of the SO8P30 and SO8P40 composites were mainly attributed to excessive PCS were added to the composites. The shrinkage of PCS during sintering leaded to the poor densification of composite. So the fiber/matrix interfacial bonding was too weak to effectively transfer load from matrix to fibers, the fracture behavior of the composites showed a completely brittle fracture. The result showed that the fiber/matrix interphase characteristics played a key role in controlling mechanical properties of the composites.

The SEM fracture surfaces images of the SO8P20 composites sintered at 1800 °C are shown in Fig. 8. They showed that the prevalent toughening mechanism operating in the composites was the debonding and pullout of the fibers. A smooth surface of the pullout fiber from the SO8P20 composites suggested suitable interphase and temperature for this kind of composites. It was expected that the liquid-phase and sintering temperature did not result in degradation of the carbon fiber.

4. Conclusions

The short-carbon-fiber-reinforced SiC composites which were prepared by hot-pressing with PCS as precursor polymer and $MgO–Al_2O_3–Y_2O_3$ as sintering additives can be densified at a relatively low temperature of 1800 °C via the liquid-phase-sintering mechanism. The highest mechanical properties were obtained for the composites with 20 wt.% PCS content. Amorphous interphase in these composites can improve the fiber/matrix bonding. The nano-PCS-derived SiC could improve the relative density of the composites. The present study confirms the fiber/matrix interphase characteristics play a key role in controlling mechanical properties of the fiber-reinforced composites.

Acknowledgments

The authors would like to thank Prof. Q.C. Meng for his excellent TEM work. The authors also express their appreciation to Prof. J.C. Rao and Prof. Y.J. Wang for their valuable comments and advice.

References

[1] C. Rospars, J.L. Chermant, P. Ladevèze, Mater. Sci. Eng. A 250 (1998) 264–269.
[2] J.S. Lee, M. Imai, T. Yano, Mater. Sci. Eng. A 339 (2003) 90–95.
[3] K. Jian, Z.H. Chen, Q.S. Ma, H.F. Hu, W.W. Zheng, Ceram. Int. 33 (2007) 905–909.
[4] J.S. Lee, T. Yano, J. Eur. Ceram. Soc. 24 (2004) 25–31.
[5] Y.Z. Zhu, Z.R. Huang, S.M. Dong, M. Yuan, D.L. Jiang, Ceram. Int. 34 (2008) 1201–1205.
[6] J.J. Brennan, Mater. Sci. Eng. A 126 (1990) 203–223.
[7] J.J. Brennan, Acta Mater. 48 (2000) 4619–4628.
[8] J.S. Lee, K. Yoshida, T. Yano, J. Ceram. Soc. Jpn. 110 (2002) 981–985.
[9] K. Jian, Z.H. Chen, Q.S. Ma, W.W. Zheng, Mater. Sci. Eng. A 390 (2005) 154–158.
[10] X.L. He, Y.K. Guo, Y. Zhou, D.C. Jia, Mater. Charact. 59 (2008) 1771–1775.
[11] X.B. He, X.M. Zhang, C.R. Zhang, Mater. Sci. Eng. A 284 (2000) 211–218.
[12] G. Boitier, J.L. Chermant, J. Vicens, Mater. Sci. Eng. A 289 (2000) 265–275.
[13] C.C. Zhou, C.R. Zhang, H.F. Hu, Y.D. Zhang, Z.Y. Wang, Mater. Sci. Eng. A 488 (2008) 569–572.
[14] Y.W. Kim, J.G. Lee, J. Mater. Sci. 27 (1992) 4746–4750.
[15] J.L. Chermant, G. Boitier, S. Darzens, G. Farizy, J. Vicens, J.C. Sangleboeuf, J. Eur. Ceram. Soc. 22 (2002) 2443–2460.
[16] X.L. He, Y. Zhou, D.C. Jia, Y.K. Guo, Ceram. Int. 32 (2006) 929–934.
[17] G. Boitier, J. Vicens, J.L. Chermant, Scripta Mater. 37 (1997) 1923–1929.
[18] E. Bouillon, F. Langlais, R. Pailler, R. Naslain, F. Cruege, P.V. Huong, J.C. Sarthou, A. Delpuech, C. Laffon, P. Lagarde, M. Monthioux, A. Oberlin, J. Mater. Sci. 26 (1991) 1333–1345.
[19] J.J. Brennan, M.C. Gerald, Mater. Sci. Eng. A 162 (1993) 53–72.